Received: 11 February 2019 | Revised: 3 June 2019 | Accepted: 17 June 2019

DOI: 10.1111/gcb.14744

PRIMARY RESEARCH ARTICLE

Global Change Biology WILEY

Negative feedback processes following drainage slow down permafrost degradation

Mathias Göckede[1] | Min Jung Kwon[1,2] | Fanny Kittler[1] | Martin Heimann[1,3] | Nikita Zimov[4] | Sergey Zimov[4,5]

[1]Max Planck Institute for Biogeochemistry, Jena, Germany

[2]Korea Polar Research Institute, Incheon, South Korea

[3]Institute for Atmospheric and Earth System Research (INAR)/Physics, University of Helsinki, Helsinki, Finland

[4]North-East Scientific Station, Pacific Institute for Geography, Far-East Branch, Russian Academy of Sciences, Cherskii, Russia

[5]Far Eastern Federal University, Vladivostok, Russia

Correspondence
Mathias Göckede, Max Planck Institute for Biogeochemistry, Hans-Knöll-Straße 10, 07745 Jena, Germany.
Email: mathias.goeckede@bgc-jena.mpg.de

Funding information
Horizon 2020 Framework Programme, Grant/Award Number: 727890 and 773421; AXA Research Fund, Grant/Award Number: PDOC_2012_W2; Seventh Framework Programme, Grant/Award Number: 282700 and PCIG12-GA-201-333796; Bundesministerium für Bildung und Forschung, Grant/Award Number: 03G0836G and 03F0764D

Abstract

The sustainability of the vast Arctic permafrost carbon pool under climate change is of paramount importance for global climate trajectories. Accurate climate change forecasts, therefore, depend on a reliable representation of mechanisms governing Arctic carbon cycle processes, but this task is complicated by the complex interaction of multiple controls on Arctic ecosystem changes, linked through both positive and negative feedbacks. As a primary example, predicted Arctic warming can be substantially influenced by shifts in hydrologic regimes, linked to, for example, altered precipitation patterns or changes in topography following permafrost degradation. This study presents observational evidence how severe drainage, a scenario that may affect large Arctic areas with ice-rich permafrost soils under future climate change, affects biogeochemical and biogeophysical processes within an Arctic floodplain. Our in situ data demonstrate reduced carbon losses and transfer of sensible heat to the atmosphere, and effects linked to drainage-induced long-term shifts in vegetation communities and soil thermal regimes largely counterbalanced the immediate drainage impact. Moreover, higher surface albedo in combination with low thermal conductivity cooled the permafrost soils. Accordingly, long-term drainage effects linked to warming-induced permafrost degradation hold the potential to alleviate positive feedbacks between permafrost carbon and Arctic warming, and to slow down permafrost degradation. Self-stabilizing effects associated with ecosystem disturbance such as these drainage impacts are a key factor for predicting future feedbacks between Arctic permafrost and climate change, and, thus, neglect of these mechanisms will exaggerate the impacts of Arctic change on future global climate projections.

KEYWORDS
Arctic climate change, drainage disturbance, energy redistribution, long-term effects, permafrost carbon

1 | INTRODUCTION

The Arctic is a hot spot of global climate change (Serreze, Barrett, Stroeve, Kindig, & Holland, 2009), and its future evolution counts among the largest uncertainties in our understanding of the Earth's climate system (Schuur & Abbott, 2011; Zimov, Schuur, & Chapin, 2006). The unique role of this region stems from the combination of observed (Fyfe et al., 2013) and predicted (IPCC, 2013) warming rates, which are higher than the global average, with an enormous permafrost carbon pool (Hugelius et al., 2014; Schuur et al., 2015) at risk of degradation (Schuur et al., 2013). The net impact of Arctic warming on permafrost carbon pool sustainability is strongly moderated by associated shifts in factors such as vegetation community structure (van der Kolk, Heijmans, van Huissteden, Pullens, & Berendse, 2016; Liang et al., 2018), snow cover dynamics (Chen, Liang, & Cao, 2016), or hydrology (Andresen & Lougheed, 2015; Jorgenson et al., 2013; Lupascu et al., 2014).

With water constituting a dominant control on Arctic ecosystem functionality (Lupascu et al., 2014), disturbing prevalent hydrologic conditions may substantially reshape feedback processes between permafrost carbon and climate change (Christiansen et al., 2017). Here, pathways include altered precipitation patterns (Bintanja & Andry, 2017; Bintanja & Selten, 2014), or lateral redistribution of water linked to warming-induced topographical changes like subsidence (Jorgenson, Shur, & Pullman, 2006; O'Donnell et al., 2012) or ice-wedge degradation (Liljedahl et al., 2016). Particularly Yedoma soils (Zimov, Davydov, et al., 2006), carbon- and ice-rich permafrost covering >1,000,000 km^2 mostly in Siberia and Alaska (Strauss et al., 2017), are highly vulnerable to warming-induced degradation, and therefore also to hydrologic disturbance.

Drying trends could enhance positive feedbacks between climate change and permafrost carbon, compared to Arctic warming alone. A synthesis of laboratory incubation studies (Schädel et al., 2016) revealed that drying of permafrost soils enhances CO_2-C losses by a factor of 3.4, compared to anaerobic incubations, clearly exceeding the effect of warming only on CO_2 emissions. Moreover, field experiments demonstrated that even minor differences in water levels exert strong effects on permafrost carbon dynamics (Zona, Lipson, Zulueta, Oberbauer, & Oechel, 2011), while severe changes can fundamentally shift ecosystem structure and exchange patterns of carbon and energy (Cooper et al., 2017; Göckede et al., 2017; Kwon et al., 2017). Commonly expected impacts of permafrost drainage include an increase in CO_2 emissions and a warming of the lower atmosphere through higher sensible heat fluxes (Göckede et al., 2017; Schuur et al., 2015).

This study demonstrates that secondary disturbance effects, mainly shifts in vegetation community composition, soil temperatures, snow cover, and thaw depth, can substantially alter the impact of Arctic drying, and reduce positive feedback mechanisms with Arctic warming. Our results build on observations from a drainage experiment on continuous permafrost at the Ambolikha site near Chersky in Northeast Siberia (Göckede et al., 2017). Parts of this predominantly waterlogged wet tussock tundra have been exposed to severe drainage since the installation of a ditch system in 2004 (Merbold et al., 2009). Since 2013, continuous year-round eddy covariance flux observations (Kittler, Heimann, et al., 2017) supplemented by flux chambers (Kwon et al., 2016, 2017) monitor carbon (CH_4, CO_2) and energy exchange processes with the atmosphere over the drained and a nearby undisturbed control area. Additional multidisciplinary observations captured structural changes in ecosystem characteristics that emerge as long-term secondary disturbance effects.

2 | MATERIALS AND METHODS

2.1 | Site description

The Ambolikha research site is located on the floodplain of the Kolyma River near Chersky (68.75°N, 161.33°E) in Northeast Siberia, Russia. The land cover is classified as wet tussock tundra, with the natural vegetation community dominated by tussock-forming sedges (*Carex appendiculata* and *lugens*) and cotton grasses (*Eriophorum angustifolium*; Kwon et al., 2016). Soils are characterized by an organic peat layer (0.15–0.2 m) overlaying alluvial mineral soils (silty clay; Corradi, Kolle, Walter, Zimov, & Schulze, 2005). The long-term mean annual air temperature is −11°C, and annual precipitation sums up to 197 mm on average (Göckede et al., 2017). During the snow melt period (May/June), the collected meltwater from the local area, in combination with backing up of regional meltwater by ice dams on the Kolyma river, usually results in minor flooding, with standing water up to 0.5 m aboveground level.

In fall of 2004, a circular drainage ditch with a diameter of 200 m and an outlet channel to the nearby Ambolikha river was installed (Merbold et al., 2009). Following the spring flooding, the improved lateral drainage created dry soil layers near the surface for the largest part of the growing season within the affected area, as opposed to predominantly inundated surfaces in the undisturbed sections. Starting July 2013, we continuously monitored exchange fluxes between the terrestrial ecosystem and the atmosphere within two treatment areas at a distance of approximately 600 m: The drainage section, and a nearby control section that was not affected by the ditch system. The immediate impact of the drainage (Merbold et al., 2009) as well as the long-term effects of sustained drier conditions on carbon fluxes (Kittler et al., 2016; Kwon et al., 2016, 2017), energy fluxes (Göckede et al., 2017), and ecosystem structure (Göckede et al., 2017; Kwon et al., 2017) have been studied in detail.

2.2 | Eddy covariance instrumentation and data processing

Treatment and control areas were equipped with eddy covariance towers (FLUXNET codes: RU-Che (drainage), RU-Ch2 (control)), featuring a heated sonic anemometer (uSonic-3 Scientific, METEK GmbH) at heights of 4.9 and 5.1 m for drainage and control towers, respectively, and two separate gas analyzers (Kittler, Eugster, et al., 2017). The default trace gas data were provided by closed

path analyzers (FGGA, Los Gatos Research Inc.) for $CH_4/CO_2/H_2O$, with air drawn through a sampling line (heated and insulated 6.2 mm Eaton Synflex decabon at a length of 16 m and 13 m for drainage and control towers, respectively) by an external vacuum pump (N940, KNF Neuberger GmbH). For extended timeframes without closed path data coverage, gaps were filled by observations from an open-path backup system (LI-7500, LI-COR Biosciences Inc.) for CO_2/H_2O flux densities.

High-frequency raw data acquisition in the field was based on the software package EDDYMEAS (Kolle & Rebmann, 2007). For the processing of eddy covariance fluxes, we used the software tool TK3 (Mauder & Foken, 2015) as a well-established package (Fratini & Mauder, 2014) for the implementation of, for example, 2D coordinate rotation of the wind field, correction for spectral losses (Moore, 1986) and density fluctuations (Webb, Pearman, & Leuning, 1980), and flux data quality control (Foken & Wichura, 1996). Flux partitioning (Reichstein et al., 2005) and gap-filling were subsequently added using the R-package "REddyProc" (Wutzler et al., 2018). Regarding the treatment of effects that are particularly relevant for year-round Arctic observations, including, for example, sensor heating to prevent ice buildup, the correction of sensor self-heating effects (Burba, McDermitt, Grelle, Anderson, & Xu, 2008), or sensor malfunction at extremely low temperatures, we developed customized data filters and quality assessment measures to ensure highest data quality (Kittler, Eugster, et al., 2017). All flux budgets presented in this manuscript are based on observational datasets from the data years 2014 and 2015.

2.3 | Chamber fluxes and site characterization

Fluxes were measured based on the non-steady-state flow-through method using a cubic plexiglas chamber with 60 cm side length placed on permanently installed PVC collars with a footprint of 60 cm × 60 cm (Kwon et al., 2016, 2017). We observed in situ $CH_4/CO_2/H_2O$ trace gas mixing ratios at 1 Hz frequency using an Ultra-Portable Greenhouse Gas Analyzer (UGGA, Los Gatos Research Inc.). To minimize biases related to saturation and pressurization effects, we restricted measurement time to a maximum of 2 min. Net ecosystem exchange (NEE) was measured using a transparent chamber, and ecosystem respiration (ER; CO_2 emitted from ecosystem to atmosphere) after blocking incoming solar radiation into the chamber. Environmental conditions, such as, temperature, humidity, and pressure, were recorded inside the chamber parallel to the mixing ratio observations. Trace gas fluxes were computed based on mixing ratio gradients over time, using a bootstrapping approach (Kwon et al., 2016, 2017).

Vegetation community structure was sampled by both harvest (2013, eight plots) and the nondestructive point intercept method (2014, 20 plots; Kwon et al., 2017), and compared to a 2003 assessment based on harvesting (Corradi et al., 2005). Water tables (in 25 mm PVC pipes) and thaw depth were measured manually in parallel with flux measurements at predefined locations on the study site. Continuous soil temperature time series are based on vertical profiles at six different locations (four sites with three sensors at 4, 16, and 64 cm below surface level; two sites with six sensors at 4, 8, 16, 32, 64, and 128 cm below surface level), representing wet and dry microsites within both treatment areas.

2.4 | Energy redistribution in the lower atmosphere

We applied the approach developed by Lee et al. (2011) to quantify the intrinsic biophysical mechanisms that govern the energy transfer within the atmospheric surface layer. Their method postulates that the temperature change caused by the disturbance of an ecosystem is governed by multiple biophysical effects that may both reinforce or oppose each other:

$$\Delta T_s \approx \frac{\lambda_0}{1+f}\Delta S + \frac{-\lambda_0}{(1+f)^2} R_n \Delta f_1 + \frac{-\lambda_0}{(1+f)^2} R_n \Delta f_2, \quad (1)$$

$$f = \frac{\rho C_p}{4 r_a \sigma T_s^3}\left(1+\frac{1}{\beta}\right), \quad (2)$$

$$\Delta f_1 = -\frac{\rho C_p}{4\sigma T_s^3 r_a}\left(1+\frac{1}{\beta}\right)\frac{\Delta r_a}{r_a}, \quad (3)$$

$$\Delta f_2 = -\frac{\rho C_p}{4\sigma T_s^3 r_a}\left(\frac{\Delta\beta}{\beta^2}\right), \quad (4)$$

where T_s [K] is the surface temperature, λ_0 [K/(W/m^2)] is the temperature sensitivity resulting from longwave radiation feedback, f [-] is the energy redistribution factor, S [W/m^2] is the net shortwave radiation, R_n [W/m^2] is the net radiation, ρ [kg/m^3] is the air density, C_p [J kg^{-1} K^{-1}] is the specific heat of air at constant pressure, σ [W m^{-2} K^{-4}] is the Stephan–Boltzmann constant, r_a [s/m] is the aerodynamic resistance, and β [-] is the Bowen ratio, that is, the ratio of sensible to latent heat fluxes. All deltas (Δ) denote differences between disturbed and undisturbed ecosystem properties.

The three terms on the right-hand side of Equation (1) represent the radiative forcing associated with albedo change, energy redistribution linked to shifts in aerodynamic roughness of the surface, and energy redistribution linked to shifts in the Bowen ratio, respectively. The driving force behind the resulting temperature change is the shift in energy input mostly driven by albedo (represented by ΔS and R_n), but energy redistribution (represented by f) has a strong moderating effect. The direct albedo effect (first term on Equation (1) right-hand side) is usually strongly dampened by f. A trend toward higher Bowen ratios (third term on Equation (1) right-hand side), that is, a relative increase in sensible heat fluxes compared to the latent heat flux rates, induces positive changes on surface temperatures. However, an effective dissipation of heat away from the surface, triggered by higher aerodynamic roughness lengths due to higher vegetation, can draw down the net impact of the excess sensible heat. Consequently, all factors are closely connected, and strongly influenced by shifts in vegetation properties such as plant height or albedo.

2.5 | Data handling and uncertainty assessment

Eddy covariance flux data uncertainty at 30-min resolution was assessed using well-established concepts (Aubinet, Vesala, & Papale, 2012) that split the total error into random and systematic errors. Since for this study only flux differences between two equally equipped eddy covariance systems with uniform data processing were employed, we could rule out systematic error effects on the resulting flux budgets (Göckede et al., 2017). Random error assessment was based on quantification of turbulent sampling errors and instrument errors from the software package TK3 (Mauder & Foken, 2015), while footprint errors (Rannik, Peltola, & Mammarella, 2016) were neglected since both towers are exposed to almost the same wind field. Adding uncertainty assessments for the gap-filled flux values (Reichstein et al., 2005), aggregated errors of the ensemble averaged fluxes were computed (Rannik et al., 2016) for the budgets of NEE, CH_4, H, and LE.

For the determination of errors in the CO_2 component fluxes gross primary productivity (GPP; photosynthetic CO_2 uptake by plants) and ER, in a first step, the random uncertainties determined for NEE were split up depending on the relative magnitude of both components. A systematic error linked to potential biases in the flux partitioning algorithm (Reichstein et al., 2005) was determined based on a direct intercomparison of measured NEE and computed ER under low-light nighttime conditions (Rg < 10 W/m^2), separately for each tower. The ratio of the average deviation to the mean ER flux rate yielded the relative flux errors per tower (drainage tower: 14.2%; control tower: 11.9%). Since potential biases in ER would be directly balanced by corresponding biases in GPP, the same error was applied to both component fluxes. The combination of random and systematic errors then yielded the total error for GPP and ER.

The error assessment for "slow" meteorological observations was based on the direct comparison of high-quality datasets between both towers at daily resolution using the so-called paired tower equation (Aubinet et al., 2012). Since towers are located only ~600 m apart, for most parameters, similar observations could be expected. For the evaluation of radiation sensors, only data from incoming radiation were used for this assessment, since surface conditions have changed considerably as a consequence of drainage, therefore also altering reflected radiation. This approach was used to derive random errors of daily averaged observations of shortwave radiation (±1.75 W/m^2), longwave radiation (±1.62 W/m^2), air temperature (±0.14 K), air pressure (±0.19 hPa), and air density (±0.0012 kg/m^3). For the uncertainty assessment in roughness length differences between towers, lower and upper error bounds were set as the 5th and 95th percentile of the distribution of roughness lengths assessed through flux–profile relationships during neutral stratification on a monthly basis.

Computation of energy redistribution, resulting in temperature differences in the lower atmosphere that can be attributed to albedo, roughness, and Bowen ratio effects (see above), was based on daily averaged meteorological input. For the determination of monthly or seasonal aggregated values, the lowest and highest, respectively, 10% of daily results were excluded to reduce the impact of outliers, and values between the 10th and 90th percentile were subsequently used for averaging. Uncertainty assessment for the energy redistribution results is based on propagating the errors of the individual input parameters as outlined above. Here, the computation of monthly or seasonally aggregated errors uses all available daily errors, that is, no outliers were excluded in the process.

3 | RESULTS

3.1 | Drainage effect on ecosystem structure

As the primary drainage effect, lowered soil water levels led to dry top soils in most parts of the affected area during the growing

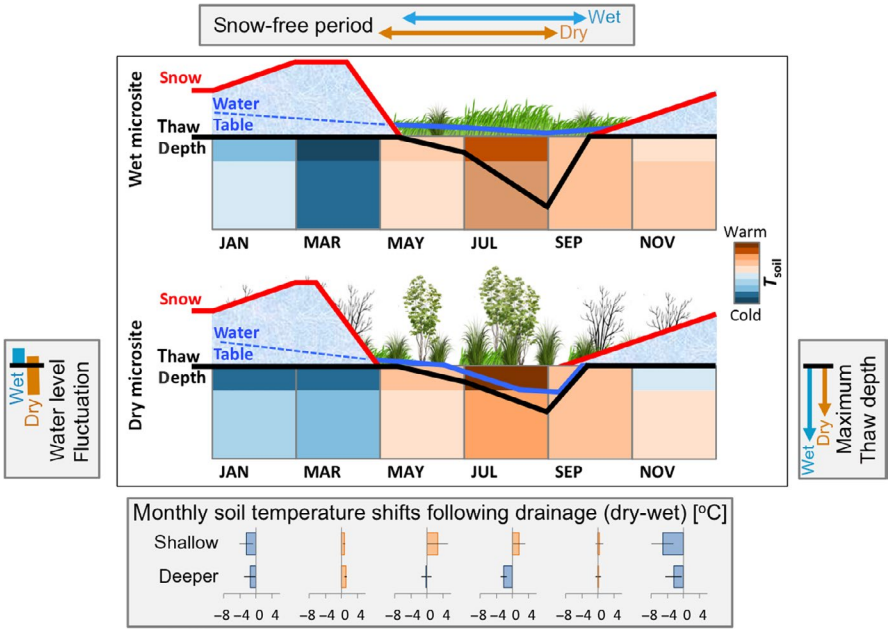

FIGURE 1 Schematic representation of shifts in permafrost ecosystem characteristics following sustained drainage. Compared to the natural conditions (wet microsite, top panel), the disturbed conditions (dry microsite, bottom panel) features a significantly lower water table (blue line) during the summer season. This triggers secondary effects, including taller vegetation, shifts in snow cover (red line), changes in soil thermal regime that differ over the course of the year (colored boxes and differences in 2-month average temperatures in bottom breakout box, both separating shallow (0–16 cm) and deep (>16 cm) soil layers), and finally a reduction in thaw depth (black line)

season (Göckede et al., 2017; Kwon et al., 2016), replacing the previous waterlogged conditions (Figure 1, blue lines, left breakout box). Following this immediate disturbance impact, several secondary changes in ecosystem properties have emerged:

1. *Soil thermal regime*: The low heat capacity in the dry organic topsoil layer (0–15 cm) amplified the fluctuations of soil temperatures near the surface, leading to warmer conditions in summer and much colder temperatures in early winter (colored boxes and bottom breakout box in Figure 1). At the same time, the reduced thermal conductivity, linked to the large fraction of air-filled pores in dry organic soils (Rouse, 2000), prevented heat transfer into deeper soil layers (>15 cm; Göckede et al., 2017). We did not conduct direct measurements of thermal conductivity, but based on values taken from Lawrence and Slater (2008), the thermal conductivity for organic peat soil ranges between 0.05 W m^{-1} K^{-1} for dry conditions and 0.55 W m^{-1} K^{-1} for saturated conditions. Based on distributed soil moisture measurements at 15 cm below surface conducted across treatments at our site, the volumetric water content varied within the range 25%–75%. Assuming 75% to represent the saturated state, a simple linear interpolation between dry and saturated thermal conductivities indicates that drainage could have lowered the value down to ~0.22 W m^{-1} K^{-1} for the driest conditions observed. The complex interplay between heat capacity and thermal conductivity implies that soil temperature offsets in deeper soil layers between drained and controls sites change signs several times over the course of the seasons (Figure 1); however, mean annual topsoil temperatures were significantly reduced in the drainage area, compared to the control section (e.g., at 16 cm depth; paired *t* test: $t = -13.85$, $p < .05$, mean difference: −0.97°C). Parts of the differences in soil temperatures between control and drained areas that Figure 1 is based on are shown in more detail in Figure 2.
2. *Vegetation community structure*: Previously dominating cotton sedges (*E. angustifolium*) were largely replaced by tussock-forming sedges (*C. appendiculata* and *lugens*) and shrubs (e.g., *Salix* ssp. and *Betula exilis*; PERMANOVA, $F = 5.22$, $p < .05$; Kwon et al., 2016). This led to an overall increase in aerodynamic roughness length (2014/15: paired *t* test: $t = -11.03$, $p < .05$) probably linked to shifts in vegetation height (Göckede et al., 2017, see also section below on energy processes). At the same time, the newly established vegetation community featured a higher overall summer albedo (as reflected in the shortwave energy budget, see below) that reflected a higher portion of the incoming solar radiation.
3. *Snow cover*: The snow-free season advanced by about 2 weeks (red line in Figure 1, top breakout box). In fall, the rougher surface in the drained area captured drifting snow (Sturm, Schimel, et al., 2005), while in spring, the parts of tall vegetation sticking out of the snow absorbed incoming radiation and thus promoted snowmelt (Sturm, Douglas, Racine, & Liston, 2005). Associated shifts in the insulation effect of the snowpack (e.g., Park, Sherstiukov, Fedorov, Polyakov, & Walsh, 2014) very likely moderated the soil temperature differences between drained and control sites.
4. *Thaw depth*: Linked to altered soil moisture and snow dynamics, we observed reductions in thaw depth in the drained areas (e.g., Jorgenson et al., 2010), compared to the wetter

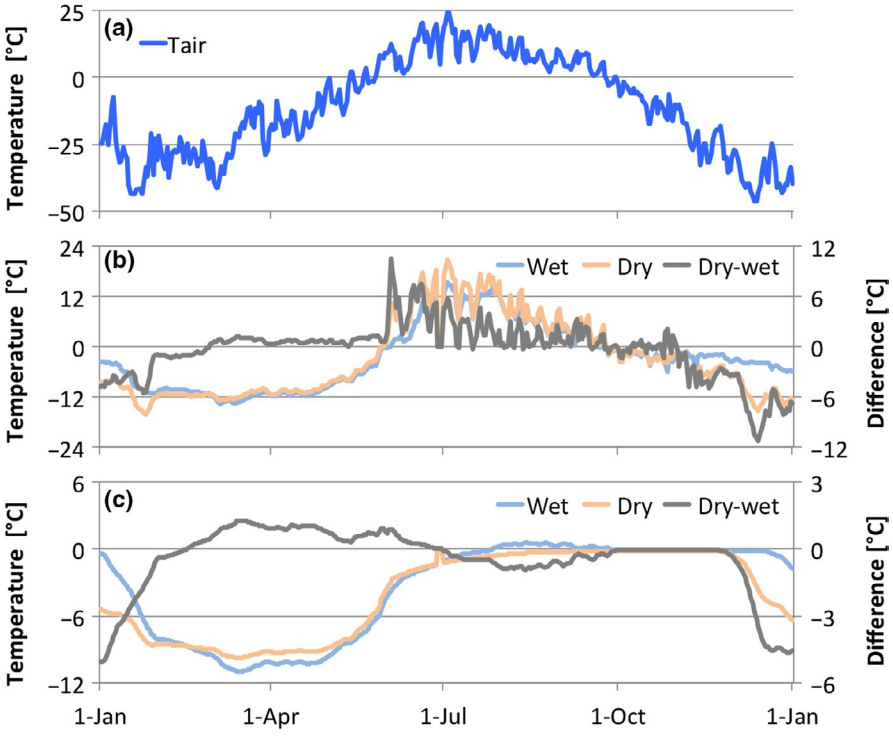

FIGURE 2 2015 time series of (a) air temperatures and soil temperatures in (b) 4 cm and (c) 64 cm below the surface. Soil temperatures are shown for a wet (light blue) and dry (orange) microsite, with their difference shown as the gray line. Please note the different temperature scales for each panel

control plots (*t* test; $t = -2.10$, $p < .05$; black lines in Figure 1, and right breakout box). This finding can be directly linked to the modified thermal properties that also changed soil temperature profiles, most importantly the reduced thermal conductivity in dry organic soil layers (Göckede et al., 2017; Kwon et al., 2016).

Detailed time series plots on soil temperature profiles, and radiation data reflecting the temporal shifts in snow cover, are given in Göckede et al. (2017). That manuscript also presents plots on the relationships between soil moisture, soil temperature, and thaw depth.

3.2 | Net drainage effect on carbon cycle processes

The above changes in ecosystem properties strongly moderated the direct impact of drainage on the exchange processes of carbon and energy between the terrestrial ecosystem and atmosphere (Figure 3). We observed an overall increase in ER by a factor of 1.35, implying a flux shift of −79.7 ± 71.6 g CO_2-C/year (Figure 4a), where negative values indicate that more carbon was released from the ecosystem to the atmosphere (Kittler, Heimann, et al., 2017). In this context, based on ER partitioning methods using natural abundance of radiocarbon, Kwon et al. (2019) determined that a strong increase in respiration within shallow soil layers (drainage: 55% of

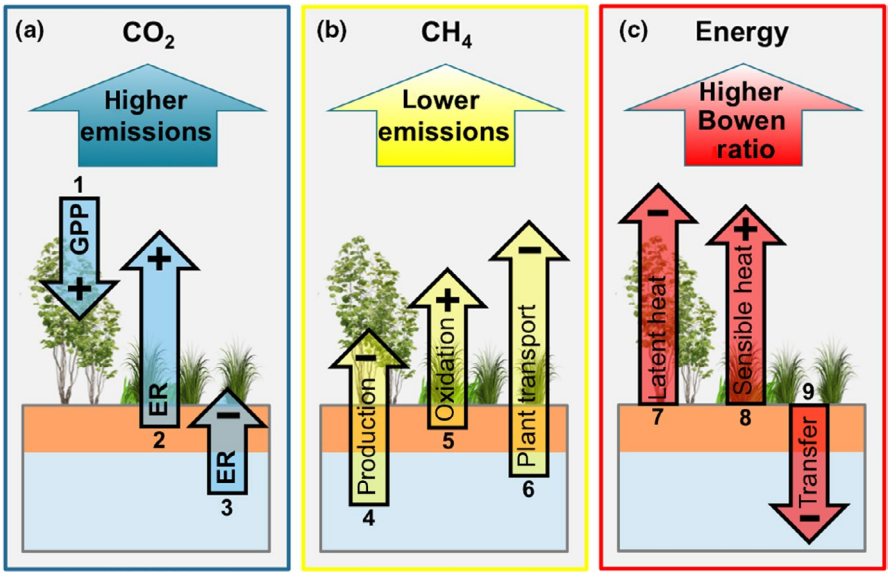

FIGURE 3 Conceptual overview on positive and negative feedbacks to climate change linked to permafrost drainage effects. (a) CO_2: The strong increase in ecosystem respiration from shallow soils (2) dominates over increases in photosynthetic uptake (1) and minor decreases in respiration from deeper soil (3), causing increased net CO_2 emissions; (b) CH_4: a decreased production in colder deep soils (4) in combination with higher oxidation in warmer and aerobic shallow soils (5) and less efficient plant transport (6) contribute to a strong decrease in CH_4 emissions; (c) energy: the reduction in latent heat fluxes (7) is almost balanced by increases in sensible heat (8), therefore shifting Bowen ratios. Reduced soil heat transfer (9) contributes to cooling permafrost soils

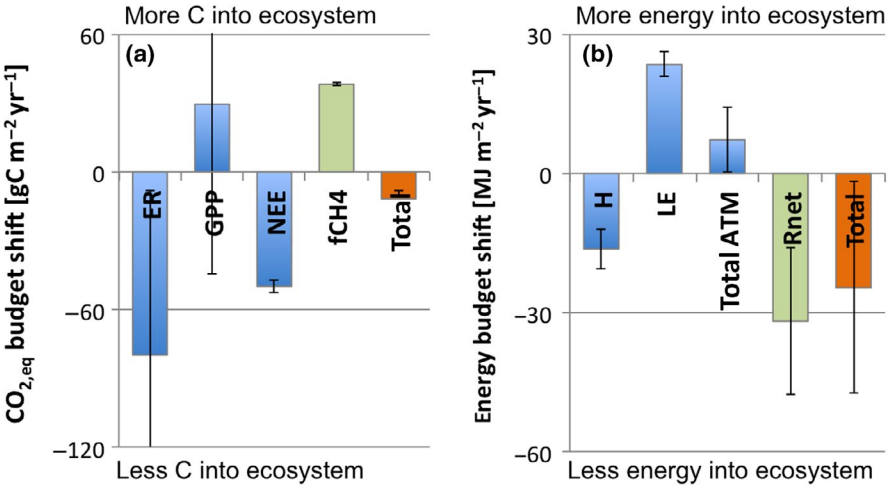

FIGURE 4 Shifts in annual budgets of carbon and energy following drainage. (a) Shifts in annual carbon budget components, converted to [$CO_{2,eq}$], as a consequence of long-term drainage disturbance at the Ambolikha observation site (ER, ecosystem respiration; GPP, gross primary productivity; NEE, net ecosystem exchange as the sum of ER and GPP; fCH_4, methane flux). (b) Shifts in annual energy budget components following drainage (H, sensible heat flux; LE, latent heat flux; total ATM, vertical energy exchange with the atmosphere as the sum of H and LE; Rnet, net radiation energy input)

total ER; control: 31%) dominated over a decrease in colder, deeper layers (drainage: 11% of total ER; control: 43%; see also left panel of Figure 3). At the same time, higher photosynthetic uptake led to a moderate increase in GPP by a factor of 1.11 (29.5 ± 74.2 g CO_2-C/year), thus counterbalancing part of the respiration losses to the atmosphere. Still, summarized shifts in net CO_2 exchange amounted to −49.9 ± 2.7 g CO_2-C/year, that is, a substantial net loss of CO_2 carbon to the atmosphere as a result of the drainage.

Methane emissions were almost halved (3.1 ± 0.05 g CH_4–C/year, factor 0.54) following drainage disturbance. Besides the shifts in soil temperatures, where particularly the colder temperatures in deeper layers may have slowed down CH_4 production, the shifts in the abundance of aerenchymatous plants that facilitate a rapid plant-mediated transport of CH_4 from these deep production layers into the atmosphere play a major role for this decrease in net emissions. Kwon et al. (2017) reported a drop in *E. angustifolium* coverage, which is the dominant aerenchymatous species at this site, from a median of 38% in the control area to just 2% in the drainage area. This shift in vegetation was accompanied by a drop in chamber-based estimates of plant-mediated CH_4 release from up to 83 mg CH_4 m^{-2} day^{-1} in wet microsites of the control section to virtually zero in dry areas. Using a global warming potential of 34, the reduced CH_4 emissions can be converted to 38.1 ± 0.6 g $CO_{2,eq}$–C/year (Figure 4a). Adding this component to the shifts in net CO_2 exchange listed above yields a minor positive feedback of −11.7 ± 3.3 g CO_2-C/year as the net drainage impact to the radiative greenhouse gas forcing induced via the change in CO_2 and CH_4 fluxes, representing an increase by a factor of only 1.05 related to the respiration budget in the control section. Accordingly, the combination of muted respiration increases linked to shifts in ecosystem structure, photosynthetic gains, and reduced CH_4 emissions add up to a close to neutral net disturbance impact on the radiative forcing from greenhouse gases.

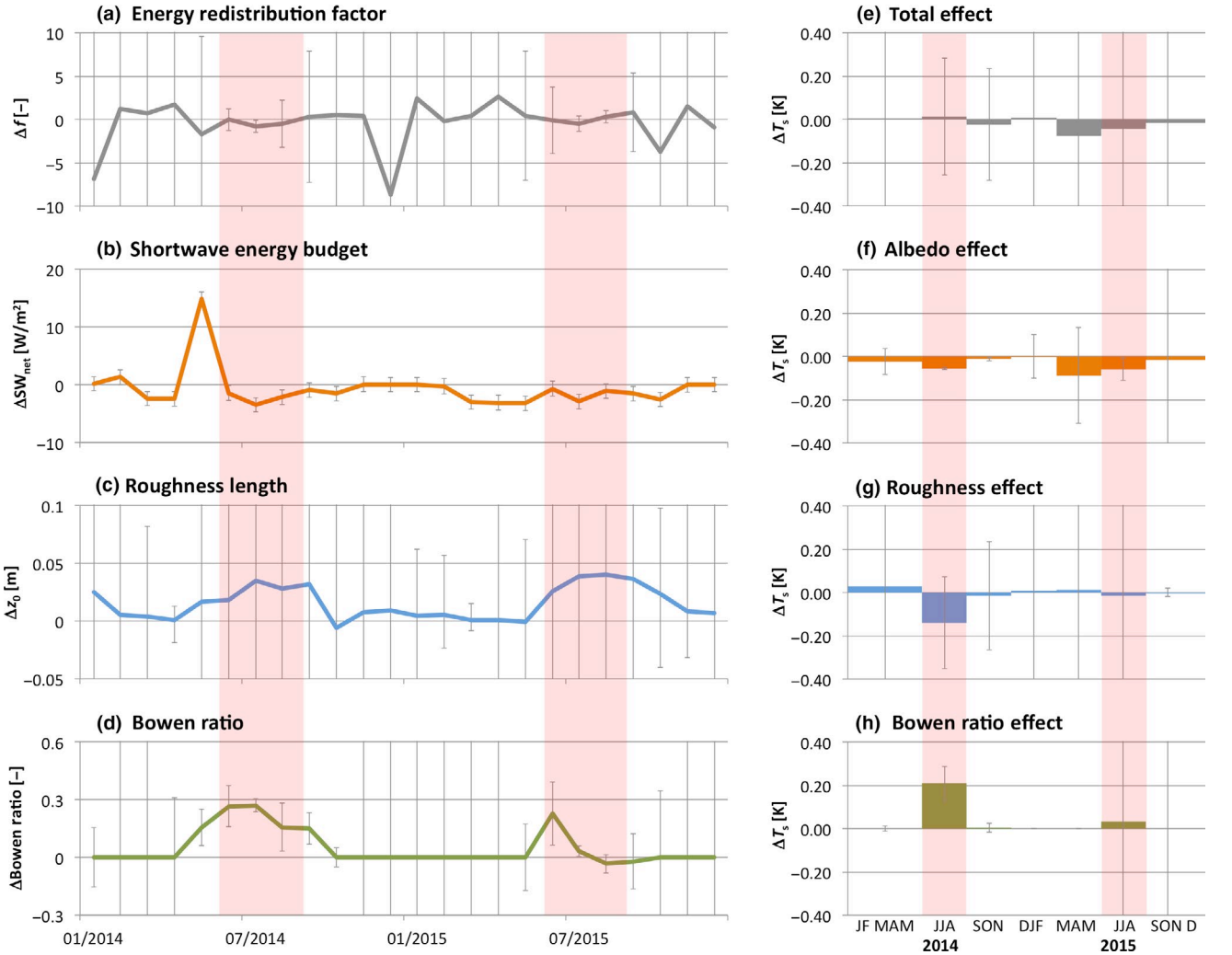

FIGURE 5 Temporal variability of shifts in biogeophysical factors (a: energy redistribution factor; b: shortwave energy budget; c: roughness length; d: Bowen ratio) and atmospheric surface layer temperatures (linked to e: all changes; f: the albedo effect; g: the roughness effect, and h: the Bowen ratio effect) after drainage disturbance. Each of the dominant biogeophysical factors controlling energy exchange between surface and lower atmosphere is linked to related shifts in atmospheric surface layer temperatures, which are aggregated by season. Results are based on a temperature response function that uses the concept of an energy redistribution factor. Growing season periods (here: calendar months June–August) are shaded in red

3.3 | Drainage impact on energy processes

Concerning the energy budget, the predominantly drier conditions following the drainage disturbance increased the energy transfer from the terrestrial ecosystem to atmosphere in form of sensible heat (H, −16.3 ± 4.3 MJ m^{-2} $year^{-1}$), while the latent heat flux (LE) was reduced (23.4 ± 2.7 MJ m^{-2} $year^{-1}$, Figure 4b). Both fluxes combined thus form a net energy gain of 7.2 ±7.0 MJ m^{-2} $year^{-1}$ to the ecosystem. This gain partly offset the substantial decrease in net radiation energy input (−31.8 ± 15.8 MJ m^{-2} $year^{-1}$) mostly associated with a higher reflection of solar radiation (albedo) of the new vegetation community. Taken together, we observed a lowered energy input into the ecosystem of −24.6 ± 22.7 MJ m^{-2} $year^{-1}$ (−0.78 ± 0.72 W/m^2) as a consequence of drainage, with the bulk of the net shift attributable to albedo changes, that is, vegetation properties.

Changes in the local energy budget (Figure 4b) hold the potential to substantially reinforce or dampen the modified radiative forcing linked to carbon cycle processes (Figure 4a, see also Hemes et al., 2018). While shifts in net energy input can warm or cool the permafrost soils, shifts in energy transfer to the lower atmosphere can change local temperature conditions. Both aspects, therefore, play a key role regarding the net feedback effect of the drainage disturbance to climate change. To estimate disturbance effects on energy transfer to the lower atmosphere, we used a temperature response function that is based on the concept of an energy redistribution factor (Lee et al., 2011) to separately quantify the feedbacks to energy exchange processes resulting from radiative forcing, roughness, and Bowen ratio:

1. An increase in albedo reduces shortwave energy input into the ecosystem (annual mean difference: −0.71 W/m^2; June–August growing season mean difference: −2.00 W/m^2; Figure 5b). Dampened by energy redistribution (Lee et al., 2011), this effect leads to a systematic cooling of lower atmosphere air temperatures (annual mean difference: −0.03 ± 0.03 K; growing season mean difference: −0.06 ± 0.03 K; Figure 5f).
2. An increase in aerodynamic roughness (annual: 0.02 m; growing season: 0.03 m; Figure 5c) improves the dissipation of sensible heat away from the surface (Lee et al., 2011). Since the net impact on air temperatures within the lower atmosphere depends on both the actual energy input and the partitioning of energy into sensible and latent heat, the roughness effect varies in sign and magnitude across the seasons (Figure 5g). Overall, the taller vegetation caused a cooling effect (annual: −0.02 ± 2.36 K; growing season: −0.09 ± 0.36 K).
3. Higher Bowen ratios (annual: 0.05; growing season: 0.15; Figure 5d), that is, shifts in energy partitioning from latent to sensible heat fluxes, reduce the removal of energy from the lower atmosphere in form of latent heat, which would be released above the atmospheric boundary layer by cloud condensation (Lee et al., 2011). Accordingly, this effect causes a net warming of the lower atmosphere (annual: 0.03 ± 0.08 K; growing season: 0.12 ± 0.30 K; Figure 5h) following drainage disturbance.

Shifts in the energy redistribution factor *f* following drainage, which were calculated using Equations (1)–(4) based on the changes in albedo, surface roughness, and Bowen ratio outlined above, varied by data year and season. The mean shifts tended toward lower *f* values integrated annually or for the summer season, respectively (−0.46; −0.28; Figure 5a). Still, we observed a minor net cooling (annual: −0.01 ± 0.21 K; growing season: −0.03 ± 0.32 K; Figure 5e) of the lower atmospheric air temperatures associated with biogeophysical mechanisms following the drainage disturbance.

4 | DISCUSSION

4.1 | Shifts in ecosystem characteristics

The overview in Figure 1 demonstrates that sustained severe drainage of a permafrost ecosystem can trigger multiple secondary change effects in ecosystem structure that are tightly connected (Göckede et al., 2017). In this context, all disturbance effects are highly dependent on the drainage severity, with shifts from wet to moist, for example, following a decrease in precipitation, having a different impact than shifts from moist to dry, as, for example, experienced through lateral drainage following ice-wedge degradation. Particularly the sensitive balance of shifts in heat capacity and thermal conductivity may lead to very different outcomes of changes in soil thermal regime depending on the degree of drainage (e.g., Rouse, Carlson, & Weick, 1992), and therefore also affect thaw depth patterns.

We found indications that the postdisturbance vegetation community structure observed at our Ambolikha site near Chersky is still adjusting to these new conditions about 12 years after the installation of the drainage ditch system. Accordingly, the observed trends toward more abundant and higher shrubs, factors that have been associated across the Arctic with feedbacks on soil temperatures (e.g., Frost, Epstein, Walker, Matyshak, & Ermokhina, 2018) and carbon cycle (e.g., Mekonnen, Riley, & Grant, 2018; Nauta et al., 2015), may continue, and further modify the net disturbance effect. Since, in addition, above- and belowground shrub growth may react differently to variability in climate forcing (Ropars et al., 2017), it is uncertain whether respiration or photosynthesis would change more due to this future development. The same holds true for energy processes: With surface roughness, albedo, and Bowen ratio all being affected by shrub growth, a net effect on energy input and redistribution cannot be predicted without further information.

The reported shifts in snow cover following disturbance, which can largely be attributed to snow–shrub interactions (Domine, Barrere, & Morin, 2016; Sturm et al., 2001), are dependent on potential shifts in the Arctic hydrological cycle. With an intensification of precipitation forecasted for large parts of the region (e.g., Bintanja & Selten, 2014), there is a potential that the disturbance impact may be muted in case higher snow packs develop. Since we do not have parallel snow measurements available within the two treatments, we cannot quantify shifts in snow depth following the

drainage disturbance. It can be speculated that the observed increases in vegetation height in dry areas also led to the accumulation of deeper snow covers, and may be contributing to the observed slightly warmer soil temperatures in the dry microsites toward the end of winter (see also Figure 2). Such increases in snow cover thus hold the potential to even outbalance the relative cooling of the dry areas in fall, which can be linked to latent heat effects due to lower soil moisture levels in these parts of the study site.

Our assessment of drainage disturbance effects on a previously wet tussock tundra ecosystem exclusively focuses on the first stages of a degradation sequence, and does not consider potential stabilization effects that may develop subsequently. Depending on the depth of the drainage channels, the progress of degradation under ongoing climate change, and also the flow conditions in the larger drainage system, an overgrowing of the channels with new vegetation and related sedimentation processes may soon reduce drainage effects (Kanevskiy et al., 2017). This type of long-term succession has not been considered within the context of this study, but may become relevant with the continuation of this disturbance experiment into the future.

Summarizing, there are many potential pathways an Arctic permafrost ecosystem may react to sustained drainage disturbance, depending on predisturbance ecosystem structure, disturbance type and severity, or time since disturbance. Changes are, moreover, dependent on prevailing climate conditions, and potential future changes therein. Accordingly, the changes observed in the context of this disturbance experiment represent just one case study, and extrapolation of detailed findings to other regions needs to be handled carefully. Still, the general mechanisms we observed should be applicable within the larger Arctic domain, particularly the important role of secondary disturbance effects on the evaluation of the net impact of a primary disturbance, in this case sustained drainage.

4.2 | Shifts in carbon fluxes

The observed overall increase in ER by a factor of 1.35 is far below the factor of 3.4 found in laboratory incubation studies (Schädel et al., 2016), which focused on isolated effects of drying or warming, and did not consider secondary disturbance effects such as, for example, shifts in vegetation community structure or soil thermal regime. Differences in methodologies, such as the inclusion of autotrophic respiration in in situ experiments that was not considered in the incubation studies, may explain parts of this discrepancy. Still, these differences can, to a large part, be linked to reduced respiration rates within the colder deeper soil layers, as documented through radiocarbon signatures (Kwon et al., 2019), which partly balanced strong increases in respiration in the dry and warm topsoil layer (Figure 3a).

The observed substantial reduction in CH_4 emissions following drainage disturbance is strongly influenced by secondary disturbance impacts linked to vegetation structure and thermal conductivity in the soil (Figure 3; see also Kwon et al., 2017): a decreased production rate in colder deep soil layers, increased oxidation in the warmer shallow soils, and reduced rates of plant-mediated transport due to a lower abundance of aerenchymatous plants. In contrast to CO_2, where the observed individual disturbance effects partly cancel each other, for CH_4 all three listed processes contributed to lowering emission rates (Figure 3b), therefore adding up to a dramatically decreased net CH_4 emission to the atmosphere following drainage.

Our findings demonstrate that changes in ecosystem structure as a slow adaptation to modified, postdisturbance environmental conditions are a key factor in assessing the net disturbance impact on carbon cycle processes. For vegetation or microbial communities and also soil nutrient pools, it may take decades to reach a representative state that allows evaluating the overall disturbance effect. In our case study, instead of a massive increase in carbon release following drainage, we obtained a near-neutral response in net carbon emissions when respiration in different soil layers, photosynthesis, and CH_4 emissions were added up. At the same time, changes in the rates of underlying processes—respiration from shallow and deep soil layers, photosynthesis, and CH_4 production and oxidation—that modified the current carbon cycling may, under future climate conditions, further reshape carbon processes (e.g., accelerated carbon turnover in the surface and shallow soil layers, but muted carbon dynamics in deep soil layers). Long-term in situ field experiments are therefore indispensable to provide data-driven insights into the intricate ecosystems responses to disturbance, and in turn inform process-based models toward a better representation of such mechanisms.

4.3 | Shifts in energy fluxes and surface layer temperature

The results summarized in Figure 5 indicate that higher aerodynamic roughness increases the energy redistribution factor *f*, while higher Bowen ratios lead to decreases. Accordingly, the net shifts in *f* change signs over the course of the seasons, depending on which of these two controls prevails at a given time. Integrating over the study period, the slightly lower average *f* values after disturbance indicate that the Bowen ratio effect dominates net changes in *f* at annual timescales, so the disturbed ecosystem has an overall reduced efficiency to dissipate energy away from the surface through intrinsic biophysical properties (Bright et al., 2017). As mentioned above, this balance is highly dependent on shifts in vegetation properties, therefore may further change with ongoing shrub growth. Still, during the observation period, shifts in ecosystem properties would have led to a minor net warming of the lower atmosphere, based on an isolated assessment of energy redistribution.

For a comprehensive assessment of the drainage impact on the energy budget, the radiative energy input into the system needs to be considered. Here, a reduced net energy input linked to albedo increases further promotes the cooling of the ecosystem, and counteracts the potential warming associated with a less efficient energy redistribution. Again, vegetation properties, in this case trends toward a surface with higher albedo following drainage, are important,

emphasizing that long-term, slow adaptation processes are a key factor for a net disturbance effect assessment.

Taken together, our results demonstrate that also in the case of the energy budget, the consideration of secondary disturbance effects substantially changes the evaluation of the net drainage effect. A simplified assessment may have focused exclusively on the immediate disturbance impact, that is, shifts from latent to sensible heat fluxes leading to higher Bowen ratios. For this single process, we found the expected increase in air temperatures linked to higher sensible heat transfer into the atmosphere after drainage, which reached monthly averaged values of >0.25 K, seemingly confirming that drainage leads to a warming of the lower atmosphere. However, also considering the shifts in biophysical properties linked to long-term changes in vegetation structure (albedo and roughness) as a secondary disturbance impact, our study demonstrates that the Bowen ratio effect is at least balanced by these counteracting factors, and as for the carbon budget leads to a near-neutral net ecosystem response to the drainage disturbance.

The interpretation of the drainage effects on the energy budget needs to consider the large uncertainties associated with the temperature effects calculated for each of the three processes summarized in the energy redistribution concept, and also for their cumulative net effect. For most of the results, the uncertainty range exceeds the absolute value of the temperature shifts associated with the drainage disturbance, and uncertainties are particularly high for annual assessments. Accordingly, the primary result here is that we did not find a significant effect of the drier surface on lower atmosphere temperatures, which would have been expected in a simplified assessment as described above, instead we found a net temperature shift that is very close to, and not significantly different from, zero.

4.4 | Representativeness of the findings

Even though the quantitative results reported in this study are site specific, our observations demonstrate the paramount importance of ecosystem structure, and shifts therein, for the evaluation of disturbance effects on climate change-carbon cycle feedbacks in the Arctic. Only multidisciplinary in situ research over long timeframes can reveal the net impact of sustained shifts in environmental conditions, which may be very different from immediate ecosystem responses to disturbance (Shaver et al., 1992). Since alterations in, for example, vegetation community or snow cover dynamics may have different characteristics in different parts of the Arctic, and thus lead to individual responses in, for example, CH_4 fluxes, albedo, or aerodynamic roughness, the net impact of all these components will be highly variable across both space and time. However, it is likely that for large parts of the Arctic, most importantly the carbon- and ice-rich soils of the Yedoma region, hydrologic disturbance linked to permafrost degradation will substantially influence feedbacks with climate warming. An isolated assessment of, for example, respiration signals or energy flux partitioning can thus only provide limited insights into the role of Arctic ecosystems in future climate scenarios.

The effect demonstrated within the context of this study, that is, drying of tundra ecosystems linked to a warming-induced topographical restructuring, only covers one side of the resulting redistribution of water. At the same time, other parts of the tundra will also become wetter, for example, the ditch systems and larger depressions where new channels, lakes, or wetlands may be created. An extrapolation of the drainage effect to the pan-Arctic, therefore, depends also on the effectuated tessellation, that is, which fraction of the degraded surface will indeed become drier, and experience changes as observed here. In the wetter areas, it can be expected that the fluxes of CH_4 and latent heat will increase, wetland vegetation will be established, and soils may tend to become warmer. Regarding an assessment on the climate impacts at regional to global scales, the total effect from both area fractions would need to be assessed.

4.5 | Implications for Arctic permafrost feedbacks with climate change

Our results demonstrate that multiple opposing effects shape the net impact of hydrologic disturbance. Soil thermal regime and vegetation community structure emerged as key elements in ecosystem property shifts that control the modified carbon and energy budgets. Adaptation to new environmental conditions may be slow, particularly regarding the vegetation, which in case of our study site was still adjusting to new conditions more than 10 years after disturbance. Instead of a dramatic increase in carbon release as found with manipulation experiments based on dry incubation of permafrost soils (Schädel et al., 2016), our in situ observations considering ecosystem structure and secondary disturbance effects yielded a near-neutral radiative forcing response following tundra drainage. In this context, particularly reduced respiration rates in deeper soil layers, strong decreases in CH_4 emissions, and a lower energy input linked to surfaces with higher albedo played a role. At the same time, reduced energy input may even lead to a cooling of the ecosystem, and together with low thermal conductivity temporarily protect the permafrost soils from further degradation. Drainage may therefore contribute to slow down decomposition of old carbon from deep soil layers, thus counterbalancing direct warming effects on permafrost carbon pools.

ACKNOWLEDGEMENTS

This work was supported through funding by the European Commission (PAGE21 project, FP7-ENV-2011, Grant Agreement No. 282700; PerCCOM project, FP7-PEOPLE-2012-CIG, Grant Agreement No. PCIG12-GA-201-333796; INTAROS project, H2020-BG-09-2016, Grant Agreement No. 727890, Nunataryuk project, H2020-BG-11-2016/17, Grant Agreement No. 773421), the German Ministry of Education and Research (CarboPerm project, Grant No. 03G0836G; KoPf project, Grant No. 03F0764D), and the AXA Research Fund (PDOC_2012_W2 campaign, ARF fellowship M. Göckede). The authors appreciate the contribution

of staff members of the Northeast Scientific Station in Chersky for facilitating the field experiments, especially Galina Zimova and Nastya Zimova. We also thank the administration and service departments within the Max-Planck-Institute for Biogeochemistry, most notably the Field Experiments & Instrumentation group, for their contributions to planning and logistics, and for supporting fieldwork activities.

CONFLICT OF INTEREST

There are no conflicts of interest.

AUTHOR CONTRIBUTIONS

MG was responsible for conceptualization of this study, development of methodologies, formal analysis, and writing of the original draft of the manuscript with input from all authors; MJK contributed analyses of soil chamber flux data, isotope analyses, and shifts in vegetation and microbial community structures; FK led the processing, quality control, and analysis of the eddy covariance datasets; MH contributed to the development of methodologies and validation of results, and funding acquisition; NZ supervised the year-round operation of the field program, and contributed to data interpretation and discussion; MH, NZ, and SAZ contributed to conceptualization of experimental design and observational infrastructure; all coauthors contributed to reviewing and editing the paper.

DATA AVAILABILITY STATEMENT

The eddy covariance flux datasets, including ancillary measurements of "slow" meteorology parameters, are available for the data years 2013–2016 in the European Fluxes Database Cluster (www.europe-fluxdata.eu) under site IDs "RU-Che" (drainage tower) and "RU-Ch2" (control tower). Data on small-scale ancillary observation can be made available by the authors upon request.

ORCID

Mathias Göckede https://orcid.org/0000-0003-2833-8401
Min Jung Kwon https://orcid.org/0000-0002-7330-2320
Fanny Kittler https://orcid.org/0000-0003-2291-6741
Martin Heimann https://orcid.org/0000-0001-6296-5113
Sergey Zimov https://orcid.org/0000-0002-0053-6599

REFERENCES

Andresen, C. G., & Lougheed, V. L. (2015). Disappearing Arctic tundra ponds: Fine-scale analysis of surface hydrology in drained thaw lake basins over a 65 year period (1948–2013). *Journal of Geophysical Research: Biogeosciences*, *120*(3), 466–479. https://doi.org/10.1002/2014JG002778

Aubinet, M., Vesala, T., & Papale, D. (Eds.). (2012). *Eddy covariance – a practical guide to measurement and data analysis*. Dordrecht, The Netherlands: Springer.

Bintanja, R., & Andry, O. (2017). Towards a rain-dominated Arctic. *Nature Climate Change*, *7*(4), 263–267. https://doi.org/10.1038/nclimate3240

Bintanja, R., & Selten, F. M. (2014). Future increases in Arctic precipitation linked to local evaporation and sea-ice retreat. *Nature*, *509*(7501), 479–482. https://doi.org/10.1038/nature13259

Bright, R. M., Davin, E., O'Halloran, T., Pongratz, J., Zhao, K., & Cescatti, A. (2017). Local temperature response to land cover and management change driven by non-radiative processes. *Nature Climate Change*, *7*(4), 296–302. https://doi.org/10.1038/nclimate3250

Burba, G. G., McDermitt, D. K., Grelle, A., Anderson, D. J., & Xu, L. K. (2008). Addressing the influence of instrument surface heat exchange on the measurements of CO_2 flux from open-path gas analyzers. *Global Change Biology*, *14*(8), 1854–1876. https://doi.org/10.1111/j.1365-2486.2008.01606.x

Chen, X. N., Liang, S. L., & Cao, Y. F. (2016). Satellite observed changes in the Northern Hemisphere snow cover phenology and the associated radiative forcing and feedback between 1982 and 2013. *Environmental Research Letters*, *11*(8), 084002. https://doi.org/10.1088/1748-9326/11/8/084002

Christiansen, C. T., Haugwitz, M. S., Priemé, A., Nielsen, C. S., Elberling, B. O., Michelsen, A., … Blok, D. (2017). Enhanced summer warming reduces fungal decomposer diversity and litter mass loss more strongly in dry than in wet tundra. *Global Change Biology*, *23*(1), 406–420. https://doi.org/10.1111/gcb.13362

Cooper, M. D. A., Estop-Aragonés, C., Fisher, J. P., Thierry, A., Garnett, M. H., Charman, D. J., … Hartley, I. P. (2017). Limited contribution of permafrost carbon to methane release from thawing peatlands. *Nature Climate Change*, *7*(7), 507–511. https://doi.org/10.1038/nclimate3328

Corradi, C., Kolle, O., Walter, K., Zimov, S. A., & Schulze, E. D. (2005). Carbon dioxide and methane exchange of a north-east Siberian tussock tundra. *Global Change Biology*, *11*(11), 1910–1925. https://doi.org/10.1111/j.1365-2486.2005.01023.x

Domine, F., Barrere, M., & Morin, S. (2016). The growth of shrubs on high Arctic tundra at Bylot Island: Impact on snow physical properties and permafrost thermal regime. *Biogeosciences*, *13*(23), 6471–6486. https://doi.org/10.5194/bg-13-6471-2016

Foken, T., & Wichura, B. (1996). Tools for quality assessment of surface-based flux measurements. *Agricultural and Forest Meteorology*, *78*(1–2), 83–105. https://doi.org/10.1016/0168-1923(95)02248-1

Fratini, G., & Mauder, M. (2014). Towards a consistent eddy-covariance processing: An intercomparison of EddyPro and TK3. *Agricultural and Forest Meteorology*, *7*(7), 2273–2281. https://doi.org/10.5194/amt-7-2273-2014

Frost, G. V., Epstein, H. E., Walker, D. A., Matyshak, G., & Ermokhina, K. (2018). Seasonal and long-term changes to active-layer temperatures after tall shrubland expansion and succession in Arctic tundra. *Ecosystems*, *21*(3), 507–520. https://doi.org/10.1007/s10021-017-0165-5

Fyfe, J. C., von Salzen, K., Gillett, N. P., Arora, V. K., Flato, G. M., & McConnell, J. R. (2013). One hundred years of Arctic surface temperature variation due to anthropogenic influence. *Scientific Reports*, *3*, 2645. https://doi.org/10.1038/srep02645

Göckede, M., Kittler, F., Kwon, M. J., Burjack, I., Heimann, M., Kolle, O., … Zimov, S. (2017). Shifted energy fluxes, increased Bowen ratios, and reduced thaw depths linked with drainage-induced changes in permafrost ecosystem structure. *Cryosphere*, *11*, 2975–2996. https://doi.org/10.5194/tc-11-2975-2017

Hemes, K. S., Eichelmann, E., Chamberlain, S. D., Knox, S. H., Oikawa, P. Y., Sturtevant, C., … Baldocchi, D. D. (2018). A unique combination of aerodynamic and surface properties contribute to surface cooling in

restored wetlands of the Sacramento-San Joaquin Delta, California. *Journal of Geophysical Research: Biogeosciences*, *123*(7), 2072–2090. https://doi.org/10.1029/2018JG004494

Hugelius, G., Strauss, J., Zubrzycki, S., Harden, J. W., Schuur, E. A. G., Ping, C.-L., … Kuhry, P. (2014). Estimated stocks of circumpolar permafrost carbon with quantified uncertainty ranges and identified data gaps. *Biogeosciences*, *11*(23), 6573–6593. https://doi.org/10.5194/bg-11-6573-2014

IPCC. (2013).*Climate change 2013: The physical science basis. Contribution of working group I to the fifth assessment report of the intergovernmental panel on climate change*. In T. F. Stocker, D. Qin, G.-K. Plattner, M. Tignor, S. K. Allen, J. Boschung, A. Nauels, Y. Xia, V. Bex, & P. M. Midgley (Eds.), Cambridge, UK and New York, NY: Cambridge University Press.

Jorgenson, M., Harden, J., Kanevskiy, M., O'Donnell, J., Wickland, K., Ewing, S., … Koch, J. (2013). Reorganization of vegetation, hydrology and soil carbon after permafrost degradation across heterogeneous boreal landscapes. *Environmental Research Letters*, *8*(3), https://doi.org/10.1088/1748-9326/8/3/035017

Jorgenson, M. T., Romanovsky, V., Harden, J., Shur, Y., O'Donnell, J., Schuur, E. A. G., … Marchenko, S. (2010). Resilience and vulnerability of permafrost to climate change. *Canadian Journal of Forest Research*, *40*(7), 1219–1236. https://doi.org/10.1139/x10-060

Jorgenson, M. T., Shur, Y. L., & Pullman, E. R. (2006). Abrupt increase in permafrost degradation in Arctic Alaska. *Geophysical Research Letters*, *33*(2), L02503. https://doi.org/10.1029/2005gl024960

Kanevskiy, M., Shur, Y., Jorgenson, T., Brown, D. R. N., Moskalenko, N., Brown, J., … Buchhorn, M. (2017). Degradation and stabilization of ice wedges: Implications for assessing risk of thermokarst in northern Alaska. *Geomorphology*, *297*(C), 20–42. https://doi.org/10.1016/j.geomorph.2017.09.001

Kittler, F., Burjack, I., Corradi, C. A. R., Heimann, M., Kolle, O., Merbold, L., … Göckede, M. (2016). Impacts of a decadal drainage disturbance on surface–atmosphere fluxes of carbon dioxide in a permafrost ecosystem. *Biogeosciences*, *13*(18), 5315–5332. https://doi.org/10.5194/bg-13-5315-2016

Kittler, F., Eugster, W., Foken, T., Heimann, M., Kolle, O., & Göckede, M. (2017). High-quality eddy-covariance CO_2 budgets under cold climate conditions. *Journal of Geophysical Research: Biogeosciences*, *122*(8), 2064–2084. https://doi.org/10.1002/2017JG003830

Kittler, F., Heimann, M., Kolle, O., Zimov, N., Zimov, S., & Göckede, M. (2017). Long-term drainage reduces CO_2 uptake and CH_4 emissions in a Siberian permafrost ecosystem. *Global Biogeochemical Cycles*, *31*(12), 1704–1717. https://doi.org/10.1002/2017gb005774

Kolle, O., & Rebmann, C. (2007). EddySoft: Dokumentation of a software package to acquire and process eddy covariance data. Retrieved from http://hdl.handle.net/11858/00-001M-0000-000E-D54C-C

Kwon, M. J., Beulig, F., Ilie, I., Wildner, M., Küsel, K., Merbold, L., … Göckede, M. (2017). Plants, microorganisms, and soil temperatures contribute to a decrease in methane fluxes on a drained Arctic floodplain. *Global Change Biology*, *23*(6), 2396–2412. https://doi.org/10.1111/gcb.13558

Kwon, M. J., Heimann, M., Kolle, O., Luus, K. A., Schuur, E. A. G., Zimov, N., … Göckede, M. (2016). Long-term drainage reduces CO_2 uptake and increases CO_2 emission on a Siberian floodplain due to shifts in vegetation community and soil thermal characteristics. *Biogeosciences*, *13*(14), 4219–4235. https://doi.org/10.5194/bg-13-4219-2016

Kwon, M. J., Natali, S. M., Hicks Pries, C. E., Schuur, E. A. G., Steinhof, A., Crummer, K. G., … Göckede, M. (2019). Drainage enhances modern soil carbon contribution but reduces old soil carbon contribution to ecosystem respiration in tundra ecosystems. *Global Change Biology*, *25*(4), 1315–1325. https://doi.org/10.1111/gcb.14578

Lawrence, D. M., & Slater, A. G. (2008). Incorporating organic soil into a global climate model. *Climate Dynamics*, *30*(2–3), 145–160. https://doi.org/10.1007/s00382-007-0278-1

Lee, X., Goulden, M. L., Hollinger, D. Y., Barr, A., Black, T. A., Bohrer, G., … Zhao, L. (2011). Observed increase in local cooling effect of deforestation at higher latitudes. *Nature*, *479*(7373), 384–387. https://doi.org/10.1038/nature10588

Liang, J., Xia, J., Shi, Z., Jiang, L., Ma, S., Lu, X., … Luo, Y. (2018). Biotic responses buffer warming-induced soil organic carbon loss in Arctic tundra. *Global Change Biology*, *24*(10), 4946–4959. https://doi.org/10.1111/gcb.14325

Liljedahl, A. K., Boike, J., Daanen, R. P., Fedorov, A. N., Frost, G. V., Grosse, G., … Zona, D. (2016). Pan-Arctic ice-wedge degradation in warming permafrost and its influence on tundra hydrology. *Nature Geoscience*, *9*(4), 312–319. https://doi.org/10.1038/Ngeo2674

Lupascu, M., Welker, J. M., Seibt, U., Maseyk, K., Xu, X., & Czimczik, C. I. (2014). High Arctic wetting reduces permafrost carbon feedbacks to climate warming. *Nature Climate Change*, *4*(1), 51–55. https://doi.org/10.1038/nclimate2058

Mauder, M., & Foken, T. (2015). *Eddy-covariance software TK3*. Retrieved from https://zenodo.org/record/20349

Mekonnen, Z. A., Riley, W. J., & Grant, R. F. (2018). 21st century tundra shrubification could enhance net carbon uptake of North America Arctic tundra under an RCP8.5 climate trajectory. *Environmental Research Letters*, *13*(5), 054029. https://doi.org/10.1088/1748-9326/aabf28

Merbold, L., Kutsch, W. L., Corradi, C., Kolle, O., Rebmann, C., Stoy, P. C., … Schulze, E.-D. (2009). Artificial drainage and associated carbon fluxes (CO_2/CH_4) in a tundra ecosystem. *Global Change Biology*, *15*(11), 2599–2614. https://doi.org/10.1111/j.1365-2486.2009.01962.x

Moore, C. J. (1986). Frequency-response corrections for eddy-correlation systems. *Boundary-Layer Meteorology*, *37*(1–2), 17–35. https://doi.org/10.1007/bf00122754

Nauta, A. L., Heijmans, M. M. P. D., Blok, D., Limpens, J., Elberling, B. O., Gallagher, A., … Berendse, F. (2015). Permafrost collapse after shrub removal shifts tundra ecosystem to a methane source. *Nature Climate Change*, *5*(1), 67–70. https://doi.org/10.1038/Nclimate2446

O'Donnell, J. A., Jorgenson, M. T., Harden, J. W., McGuire, A. D., Kanevskiy, M. Z., & Wickland, K. P. (2012). The effects of permafrost thaw on soil hydrologic, thermal, and carbon dynamics in an Alaskan peatland. *Ecosystems*, *15*(2), 213–229. https://doi.org/10.1007/s10021-011-9504-0

Park, H., Sherstiukov, A. B., Fedorov, A. N., Polyakov, I. V., & Walsh, J. E. (2014). An observation-based assessment of the influences of air temperature and snow depth on soil temperature in Russia. *Environmental Research Letters*, *9*(6), 064026. https://doi.org/10.1088/1748-9326/9/6/064026

Rannik, Ü., Peltola, O., & Mammarella, I. (2016). Random uncertainties of flux measurements by the eddy covariance technique. *Atmospheric Measurement Techniques*, *9*(10), 5163–5181. https://doi.org/10.5194/amt-9-5163-2016

Reichstein, M., Falge, E., Baldocchi, D., Papale, D., Aubinet, M., Berbigier, P., … Valentini, R. (2005). On the separation of net ecosystem exchange into assimilation and ecosystem respiration: Review and improved algorithm. *Global Change Biology*, *11*(9), 1424–1439. https://doi.org/10.1111/j.1365-2486.2005.001002.x

Ropars, P., Angers-Blondin, S., Gagnon, M., Myers-Smith, I. H., Lévesque, E., & Boudreau, S. (2017). Different parts, different stories: Climate sensitivity of growth is stronger in root collars vs. stems in tundra shrubs. *Global Change Biology*, *23*(8), 3281–3291. https://doi.org/10.1111/gcb.13631

Rouse, W. R. (2000). The energy and water balance of high-latitude wetlands: Controls and extrapolation. *Global Change Biology*, *6*, 59–68. https://doi.org/10.1046/j.1365-2486.2000.06013.x

Rouse, W. R., Carlson, D. W., & Weick, E. J. (1992). Impacts of summer warming on the energy and water-balance of wetland tundra. *Climatic Change*, *22*(4), 305–326. https://doi.org/10.1007/bf00142431

Schädel, C., Bader, M.-F., Schuur, E. A. G., Biasi, C., Bracho, R., Čapek, P., … Wickland, K. P. (2016). Potential carbon emissions dominated by carbon dioxide from thawed permafrost soils. *Nature Climate Change*, *6*(10), 950–953. https://doi.org/10.1038/nclimate3054

Schuur, E. A. G., & Abbott, B. (2011). Climate change: High risk of permafrost thaw. *Nature*, *480*(7375), 32–33. https://doi.org/10.1038/480032a

Schuur, E. A. G., Abbott, B. W., Bowden, W. B., Brovkin, V., Camill, P., Canadell, J. G., … Zimov, S. A. (2013). Expert assessment of vulnerability of permafrost carbon to climate change. *Climatic Change*, *119*(2), 359–374. https://doi.org/10.1007/s10584-013-0730-7

Schuur, E. A. G., McGuire, A. D., Schädel, C., Grosse, G., Harden, J. W., Hayes, D. J., … Vonk, J. E. (2015). Climate change and the permafrost carbon feedback. *Nature*, *520*(7546), 171–179. https://doi.org/10.1038/nature14338

Serreze, M. C., Barrett, A. P., Stroeve, J. C., Kindig, D. N., & Holland, M. M. (2009). The emergence of surface-based Arctic amplification. *Cryosphere*, *3*(1), 11–19. https://doi.org/10.5194/tc-3-11-2009

Shaver, G. R., Billings, W. D., Chapin, F. S., Giblin, A. E., Nadelhoffer, K. J., Oechel, W. C., & Rastetter, E. B. (1992). Global change and the carbon balance of Arctic ecosystems. *BioScience*, *42*(6), 433–441. https://doi.org/10.2307/1311862

Strauss, J., Schirrmeister, L., Grosse, G., Fortier, D., Hugelius, G., Knoblauch, C., … Veremeeva, A. (2017). Deep Yedoma permafrost: A synthesis of depositional characteristics and carbon vulnerability. *Earth Science Reviews*, *172*, 75–86. https://doi.org/10.1016/j.earscirev.2017.07.007

Sturm, M., Douglas, T., Racine, C., & Liston, G. E. (2005). Changing snow and shrub conditions affect albedo with global implications. *Journal of Geophysical Research*, *110*(G1), G01004. https://doi.org/10.1029/2005jg000013

Sturm, M., McFadden, J. P., Liston, G. E., Chapin, F. S., Racine, C. H., & Holmgren, J. (2001). Snow-shrub interactions in Arctic tundra: A hypothesis with climatic implications. *Journal of Climate*, *14*(3), 336–344. https://doi.org/10.1175/1520-0442(2001)014<0336:SSIIAT>2.0.CO;2

Sturm, M., Schimel, J., Michaelson, G., Welker, J. M., Oberbauer, S. F., Liston, G. E., … Romanovsky, V. E. (2005). Winter biological processes could help convert arctic tundra to shrubland. *BioScience*, *55*(1), 17–26. https://doi.org/10.1641/0006-3568(2005)055[0017:wbpchc]2.0.co;2

van der Kolk, H. J., Heijmans, M. M. P. D., van Huissteden, J., Pullens, J. W. M., & Berendse, F. (2016). Potential Arctic tundra vegetation shifts in response to changing temperature, precipitation and permafrost thaw. *Biogeosciences*, *13*(22), 6229–6245. https://doi.org/10.5194/bg-13-6229-2016

Webb, E. K., Pearman, G. I., & Leuning, R. (1980). Correction of flux measurements for density effects due to heat and water-vapor transfer. *Quarterly Journal of the Royal Meteorological Society*, *106*(447), 85–100. https://doi.org/10.1002/qj.49710644707

Wutzler, T., Lucas-Moffat, A., Migliavacca, M., Knauer, J., Sickel, K., Šigut, L., … Reichstein, M. (2018). Basic and extensible post-processing of eddy covariance flux data with REddyProc. *Biogeosciences*, *15*(16), 5015–5030. https://doi.org/10.5194/bg-15-5015-2018

Zimov, S. A., Davydov, S. P., Zimova, G. M., Davydova, A. I., Schuur, E. A. G., Dutta, K., & Chapin, F. S. (2006). Permafrost carbon: Stock and decomposability of a globally significant carbon pool. *Geophysical Research Letters*, *33*(20), L20502. https://doi.org/10.1029/2006gl027484

Zimov, S. A., Schuur, E. A. G., & Chapin, F. S. (2006). Permafrost and the global carbon budget. *Science*, *312*(5780), 1612–1613. https://doi.org/10.1126/science.1128908

Zona, D., Lipson, D. A., Zulueta, R. C., Oberbauer, S. F., & Oechel, W. C. (2011). Microtopographic controls on ecosystem functioning in the Arctic Coastal plain. *Journal of Geophysical Research*, *116*, G00I08. https://doi.org/10.1029/2009JG001241

How to cite this article: Göckede M, Kwon MJ, Kittler F, Heimann M, Zimov N, Zimov S. Negative feedback processes following drainage slow down permafrost degradation. *Glob Change Biol*. 2019;25:3254–3266. https://doi.org/10.1111/gcb.14744